

Counterstreaming electrons and ions in Pierce-like diodes

Heidrun Kolinsky and Hans Schamel

Physikalisches Institut, Universität Bayreuth, D-95440 Bayreuth, Germany

(Received 27 February 1995)

The dynamics of Pierce-like diodes is investigated for ions moving with arbitrary velocities opposite to as well as in the direction of electron propagation. By application of an integral formalism that is able to account for mobile streaming ions, equilibrium solutions for the diode in an external circuit are derived. The stability of the uniform equilibrium for the short-circuited diode and for counterstreaming species is investigated. In this case, new oscillatory unstable branches appear that destabilize the diode for all values of α , where α is the Pierce parameter. This contrasts with the diode with co-moving ions being stable for sufficiently small values of α . These new branches coincide with the Pierce-Buneman modes for initially resting ions. If $|v_{i0}|/v_{e0}$ is increased, where v_{s0} are the injection velocities ($s=e,i$), a stronger destabilization is observed for counterstreaming in comparison to co-streaming with maximum growth rate in the range of $v_{i0} \approx -2v_{e0}$ for a hydrogen plasma. It is furthermore shown that the familiar picture of waves (Fourier modes) must be substantially modified to meet the physics of bounded plasmas.

PACS number(s): 52.75.Fk, 52.90.+z, 52.35.-g, 41.85.Ja

I. INTRODUCTION

Many plasma systems used in science and technology such as Q machines or thermionic converters are beam-plasma devices exhibiting a rich variety of boundary controlled phenomena [1]. Theoretical models accounting for this circumstance are, therefore, of profound interest.

One of the basic bounded plasma models is the Pierce diode [2], which is an idealized one-dimensional model useful for low density current-carrying bounded plasmas. In the Pierce diode, a cold electron beam of density n_0 and velocity v_{e0} is emitted at the cathode at $x=0$ and completely absorbed at the anode at $x=L$. The electrodes are held at the same potential. The ions form an immobile neutralizing background. The model is electrostatic, one dimensional, and collisionless and can be considered as a first step to the theoretical description of experiments such as thermionic low pressure discharges [3,4] or magnetic box discharges. The Pierce model has also been used in the context of ion-beam neutralization for inertial confinement fusion [5,6], high power microwave sources [7], cosmic plasma flow [8,9], and p - i - n semiconductor diodes [10]. Pierce found that the uniform equilibrium of the diode is destabilized if $\alpha \equiv \omega_{pe}L/v_{e0}$ exceeds π , where $\omega_{pe} = \sqrt{n_0 e^2 / \epsilon_0 m_e}$ is the electron plasma frequency at injection and L the diode length, m_e the electron mass, e the elementary charge, and ϵ_0 the permittivity of the vacuum, respectively.

The nonlinear dynamics of the Pierce diode has been extensively studied by Godfrey [11]. External circuit effects have been incorporated in both analysis and numerical simulation by Hörhager and Kuhn [12], Lawson [13], and Crystal and Kuhn [14]. Besides direct numerical integration techniques of the basic integral equations [11,13], particle simulations of the diode have been performed mostly on the basis of the PDP1 computer code [15] giving deep insight into the nonlinear dynamics of

the simplest possible model of a bounded plasma discharge.

Finite ion mass effects have so far been incorporated into the Pierce diode model in [16–21]. The interaction of an electron beam with initially resting ions ($v_{i0}=0$) leads to an instability of the uniform equilibrium for all values of α . New growing oscillatory modes due to ion dynamics, called Pierce-Buneman modes, appear which have been experimentally verified by Iizuka *et al.* [22]. Ion dynamical effects involving arbitrary finite ion velocities have been investigated in [23–26].

The integral formulation presented in [23,24] being an extension of the one introduced and applied by Godfrey [11] and Lawson [13] offers the possibility to treat the dynamical behavior of a plasma diode in a general context. It makes use of a Lagrangian description of the active species assuming the latter to be governed by hydrodynamic equations and it permits a higher flexibility in the incorporation of boundary conditions and of the dynamics of the second species than Eulerian schemes. In [23] it is the electron dynamics that is described in a Lagrangian manner supplemented by the linearized ion dynamics, whereas in [24] the ions are treated as active particles assuming a quasistatic kinetic equation of state for the electrons. The advantage of this description is that within the limits imposed by the validity of the underlying equations the complete nonlinear dynamical behavior can be evaluated, which includes, for example, the search for equilibria in dependence on various kinds of boundary conditions or the search for bifurcations and stability regimes. Examples of its versatility have already been presented in [23] and [24], and as a special application of [23] the stability of a Pierce-like diode in case of arbitrary ion injection velocities could be investigated by the present authors [26]. The stability was shown in that paper to be controlled by the parameter $\hat{\alpha} = \alpha(1 + \hat{\mu})^{1/2}$, where α is the Pierce parameter and $\hat{\mu} = m_e v_{e0}^2 / m_i v_{i0}^2$ is

the ratio of electron and ion kinetic energy at the emitter. In addition, a generalized dispersion relation for linear electrostatic perturbations of the uniform equilibrium was established. Its evaluation exhibits several interesting features, such as the appearance of growing oscillatory modes which in the limit of initially resting ions become Pierce-Buneman modes.

In [23,26] the ions were emitted from the same electrode as the electrons, a situation that applies, for instance, to thermionic converters or to Knudsen diodes with surface ionization. There are, however, circumstances where ions enter the active diode region from an opposite direction such as in triple plasma devices or in low pressure magnetic box or linear discharges [3,4] where a residual neutral component experiences ionization in the anode region, setting free ions moving towards the electron emitting cathode. We therefore found it worthwhile to investigate this case in some detail since it is, as it turns out, not simply an extension of the already treated co-moving case, as one might perhaps expect. The essence of the present paper consists in effects generated by counterstreaming charged particles. We mention parenthetically that the Lagrangian formulation proved to be beneficial also in a pure electron diode as shown by Coutsias and Sullivan [7]. Kinetic effects (except that treated in [24]) are, however, out of the scope of a Lagrangian description and demand different treatments such as that introduced by Kuznetsov and Ender [9].

This paper is organized as follows. In Sec. II the basic formulas describing the diode dynamics are presented. The similarities and differences between the case of coinjection of electrons and ions and of counterstreaming species are emphasized. The equilibrium solutions are given in Sec. III. In the following section, the dispersion relation for counterstreaming particles is derived, numerically evaluated, and discussed. A summary completes the paper.

II. BASIC EQUATIONS

In the following the basic formulas describing the diode dynamics are presented. Both species are assumed to be cold. The electrons are injected with density n_0 at $x=0$ which is the position of the cathode (see Fig. 1). The ions are injected with equal density either at the cathode or at the anode. A Lagrangian description of the electron fluid is used. $x(t_0, t)$ represents the position of an electron fluid element at the time t , which was released from $x=0$ at the time $t_0 \leq t$. The ion fluid is treated in linear approximation, which is justified by the small mass ratio $\mu \equiv m_e/m_i \ll 1$. Ions are allowed from the outset to have an arbitrary injection velocity v_{i0} . The governing equations derived by Schamel and Maslov [23] can be kept; it makes no difference with respect to the starting equations whether the ions are injected at the anode or at the cathode. They read in normalized form

$$\ddot{x}(t_0, t) - \alpha^2(t - t_0) - \alpha^2 \int_{t_0}^t d\tau x'(\tau, t) \bar{n}_i(\tau, t) = -E_0(t), \quad (1)$$

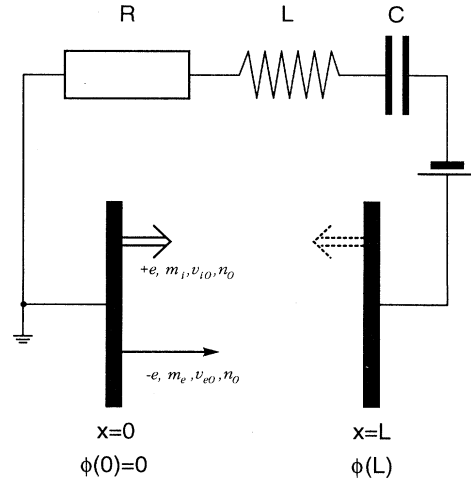


FIG. 1. The model of the generalized Pierce diode. Cold electrons are injected at the cathode ($x=0$) with density n_0 and velocity v_{e0} . Cold ions are injected with equal density and arbitrary velocity v_{i0} from the cathode (co-injection) or from the anode ($x=L$) (counterstreaming). The electrodes are connected by an external circuit consisting of a resistance R , an inductance L , and a capacity C .

$$\Xi \tilde{N}_i(t_0, t) = -\tilde{U}'_i(t_0, t), \quad (2)$$

$$\Xi \tilde{U}_i(t_0, t) = -\mu x'(t_0, t) \dot{x}(t_0, t).$$

In these equations

$$\bar{n}_i(t_0, t) = 1 + \tilde{N}_i(t_0, t) \equiv n_i[x(t_0, t), t], \quad (3)$$

$$\bar{v}_i(t_0, t) = A^{-1} + \tilde{U}_i(t_0, t) \equiv v_i[x(t_0, t), t]$$

represent the ion density and the ion velocity, respectively. The operator Ξ is defined by

$$\Xi \equiv x'(t_0, t) \partial_t + [A^{-1} - \dot{x}(t_0, t)] \partial_{t_0}. \quad (4)$$

In the following prime (overdot) means differentiation with respect to the first (second) argument, i.e., $x'(t_0, t) \equiv \partial_{t_0} x(t_0, t)$ and $\dot{x}(t_0, t) \equiv \partial_t x(t_0, t)$. The constant α denotes the Pierce parameter $\alpha = \omega_{pe} L / v_{e0}$, where $\omega_{pe} = \sqrt{n_0 e^2 / \epsilon_0 m_e}$ is the plasma frequency based on n_0 , L is the diode length, and $A = v_{e0} / v_{i0}$ is the ratio of electron and ion injection velocity. Injection of the ions at the anode leads to negative values of A . As said, up to now no difference must be made between the case of coinjection (injection of both species at the cathode) and counterstreaming electrons and ions (injection of the ions at the anode) [23,26]. $E_0(t) \equiv \bar{E}(t, t)$ denotes the electric field at $x=0$ which is generally time dependent. In [23] both Eqs. (2) were combined to yield a single second order equation for $\tilde{N}_i(t_0, t)$. This equation is, however, incomplete, since it was implicitly assumed that the operators Ξ and ∂_{t_0} commute with each other. If we use the correct commutation law, nevertheless both equations can be combined to yield a single equation for $\tilde{N}_i(t_0, t)$:

$$\begin{aligned}
x'(t_0, t) \Xi^2 \tilde{N}_i(t_0, t) - \{x''(t_0, t)[1/A - \dot{x}(t_0, t)]^2 \\
+ 2x'(t_0, t)\dot{x}'(t_0, t)[1/A - \dot{x}(t_0, t)] \\
+ [x'(t_0, t)]^2 \ddot{x}(t_0, t)\} \tilde{N}_i'(t_0, t) \\
= \mu [x'(t_0, t)]^2 \ddot{x}'(t_0, t) . \quad (5)
\end{aligned}$$

The coupled system (1) and (5) hence describes the electron dynamics nonlinearly and ion dynamics linearly. Two further boundary conditions must in addition be fulfilled [11,13,23,24].

(i) The transit time condition, i.e., the fact that an electron fluid element reaches $x=1$ at the time t when it has been released from $x=0$ at $t_0=t-T$:

$$x(t-T, t) = 1 , \quad (6)$$

where T is the transit time. Alternatively, Eq. (6) can be considered as the defining equation of the Lagrangian auxiliary quantity T .

(ii) The external-circuit equation as derived by Kuhn and Hörhager [27] and transferred by Lawson [13] into

$$\begin{aligned}
\int_0^1 E(x, t) dx = \int_{t_0}^{t-T} \tilde{E}(t_0, t) x'(t_0, t) dt_0 \\
= - \left[\bar{L} \frac{d^2}{dt^2} + R \frac{d}{dt} + \frac{1}{C} \right] E_0(t) \quad (7)
\end{aligned}$$

has to be fulfilled, R , \bar{L} , and C are the normalized values of an external resistance, inductivity, and capacity. They are given by

$$C \leftarrow C' = \frac{C}{C_0} = \frac{C}{\epsilon_0 A / L} ,$$

$$R \leftarrow R' = R C_0 \frac{v_{e0}}{L} ,$$

$$\bar{L} \leftarrow \bar{L}' = \bar{L} C_0 \frac{v_{e0}^2}{L^2} .$$

As long as there is no return of electron-fluid elements and as long as the ions do not accumulate, which would cause a breakdown of the linearized ion dynamics, the coupled system of Eqs. (1) and (5) together with the boundary conditions (6) and (7) describes the spatio-temporal dynamics of the diode. If there is no virtual cathode, Eq. (1) is a suitable description of the nonlinear electron dynamics. Only the electric field at the cathode $E_0(t)$ and the ion density $n_i(t_0, t)$ must be determined. If it is necessary to treat the ion dynamics nonlinearly such as in the case of an ion accumulation, Eq. (1) must be supplemented by the ion continuity and the ion momentum equations instead of (5). These cases seem only accessible to numerical methods. Here we focus our interest on the analytically solvable problem of linearized ion dynamics which in view of $\mu \ll 1$, the small mass ratio, is a reasonable restriction.

For a small electric field E_0 at the cathode we look for an analytic solution of the coupled equation system (1) and (5) by the ansatz

$$x(t_0, t) = X(t_0, t) + Y(t_0, t) , \quad (8)$$

where $X(t_0, t)$ is $O(1)$, satisfying already the boundary conditions

$$x(t_0, t_0) = 0, \quad \dot{x}(t_0, t_0) = 1, \quad x'(t_0, t_0) = -1 . \quad (9)$$

The solution of $O(1)$ is found to be $X(t_0, t) = t - t_0$. It represents the unperturbed motion of the electrons. The deviation $Y(t_0, t)$ from straight line orbit results from a nonzero electric field and from the mobility of the ions. $Y(t_0, t)$ is assumed to be $O(\epsilon)$. The contribution to $O(\epsilon)$ of Eq. (1) is

$$\ddot{Y}(t_0, t) + \alpha^2 Y(t_0, t) + \alpha^2 \int_{t_0}^t d\tau \tilde{N}_i(\tau, t) = -E_0(t) . \quad (10)$$

$\tilde{N}_i(t_0, t)$ follows from the lowest order of (5) which becomes

$$\ddot{\tilde{N}}_i(t_0, t) + 2\mathcal{A} \dot{\tilde{N}}_i'(t_0, t) + \mathcal{A}^2 \tilde{N}_i''(t_0, t) = -\mu \ddot{Y}'(t_0, t) , \quad (11)$$

where \mathcal{A} is defined by $\mathcal{A} \equiv (1 - A^{-1})$. The equations are the same whether the species move in the same direction or in opposite directions. The range of \mathcal{A} is given by $-\infty < \mathcal{A} \leq 1$ in the case of co-injection. $\mathcal{A} = 1$ stands for zero ion velocity, denoted as initially resting ions and $\mathcal{A} = 0$ for equal values of the injection velocities in this case. Counterstreaming of the species leads to a negative \mathcal{A} and thus \mathcal{A} is in the range of $1 \leq \mathcal{A} < +\infty$. The difference arises from the boundary conditions, as we will see. The last equation can be written as

$$(\partial_t + \mathcal{A} \partial_{t_0})^2 \tilde{N}_i(t_0, t) = -\mu \partial_{t_0} \partial_t^2 Y(t_0, t) . \quad (12)$$

From a differentiation of Eq. (10) with respect to t_0 , we obtain

$$\tilde{N}_i'(t_0, t) = \frac{1}{\alpha^2} \partial_{t_0} (\partial_t^2 + \alpha^2) Y(t_0, t) . \quad (13)$$

Combination of both equations leads to a differential equation for the deviation of the ion fluid density from the injection density:

$$[(\partial_t^2 + \alpha^2)(\partial_t + \mathcal{A} \partial_{t_0})^2 + \alpha^2 \mu \partial_t^2] \tilde{N}_i(t_0, t) = 0 \quad (14)$$

or alternatively to a differential equation for $Y(t_0, t)$:

$$\partial_{t_0} [(\partial_t^2 + \alpha^2)(\partial_t + \mathcal{A} \partial_{t_0})^2 + \alpha^2 \mu \partial_t^2] Y(t_0, t) = 0 , \quad (15)$$

having in common the same linear differential operator in brackets. This operator commutes with ∂_{t_0} . In the equations still no difference must be made concerning the direction of the ion velocity, whereas the boundary conditions will be different. Furthermore, vanishing density and velocity perturbations of both species at the injection planes are assumed. This means $\delta n_e = 0$ and $\delta v_e = 0$ for all times t at $x=0$ and the electron injection conditions read

$$\begin{aligned}
Y(t_0, t_0) = 0, \quad \dot{Y}(t_0, t_0) = 0 , \\
Y'(T_0, t_0) = -E_0(t_0) . \quad (16)
\end{aligned}$$

The condition of zero ion density perturbations becomes in the case of counterstreaming electrons and ions ($t_0 = t - T$)

$$\tilde{N}_i(t-T, t) = 0 \quad (17)$$

instead of

$$\tilde{N}_i(t_0, t_0) = 0$$

which applies for co-moving species. From the ion continuity and momentum equation [23] in the limit $t_0 \rightarrow t - T$ (counterstreaming) and $t \rightarrow t_0$ (co-injection) can be derived

$$\tilde{N}_i'(t-T, t) = \hat{\mu} \ddot{x}(t-T, t) x'(t-T, t) \quad (18)$$

and

$$\tilde{N}_i'(t_0, t_0) = \hat{\mu} E_0(t_0),$$

respectively, using the boundary conditions $\ddot{x}(t_0, t_0) = -E_0(t_0)$ and $x'(t_0, t_0) = -1$.

III. EQUILIBRIUM SOLUTIONS

In the preceding section we have shown how the boundary conditions are altered if one switches from co- to counterstreaming ions. This change has important consequences as it influences the method of solution, as will be demonstrated in this section. For the sake of clarity we simultaneously treat both cases and point out the differences. In the following the subscript A refers to ions injected at the anode (counterstreaming) whereas the subscript C refers to ions injected at the cathode (co-injection). If subscripts are missing the equation is valid for both situations.

Small amplitude equilibria solutions with $E_0 = \text{const}$ of $O(\epsilon)$ can be found as follows. For equilibria, the t_0 and t dependency is simply given by $X = t - t_0$, which reflects the time invariance. The differential equations are transformed with $\mathcal{Y}(X) \equiv Y(t_0, t)$, $\mathcal{N}(X) \equiv \tilde{N}_i(t_0, t)$ and $\partial_{t_0} \rightarrow -\partial_X$, $\partial_t \rightarrow \partial_X$ into

$$-\partial_X \hat{\mathcal{L}} \mathcal{Y}(X) = 0 \quad (19)$$

and

$$\hat{\mathcal{L}} \mathcal{N}(X) = 0 \quad (20)$$

with the linear differential operator $\hat{\mathcal{L}} \equiv \partial_X^2 (\partial_X^2 + \hat{\alpha}^2)$. Correspondingly, the deviation of the ion fluid density is given by

$$\mathcal{N}(X) = -\frac{1}{\hat{\alpha}^2} \partial_X (\partial_X^2 + \alpha^2) \mathcal{Y}(X) \quad (21)$$

and

$$\partial_X^2 \mathcal{N}(X) = \hat{\mu} \partial_X^3 \mathcal{Y}(X). \quad (22)$$

The boundary conditions read in the case of counterstreaming electrons and ions

$$\mathcal{Y}(0) = 0, \quad \mathcal{Y}'(0) = 0, \quad \mathcal{Y}''(0) = -E_0, \quad (23)$$

$$\mathcal{N}_A(T) = 0, \quad \mathcal{N}'_A(T) = \hat{\mu} \mathcal{Y}''(T) [1 + \mathcal{Y}'(T)]. \quad (24)$$

In the case of co-injection, T has to be substituted by 0. In order to learn how the differences in the boundary conditions affect the analysis we first treat the case of co-

injection. After a threefold integration, the differential equation (19) for $\mathcal{Y}(X)$ becomes

$$\mathcal{Y}''_C(X) + \hat{\alpha}^2 \mathcal{Y}_C(X) = c_1 + c_2 X + c_3 X^2. \quad (25)$$

The constants c_1 , c_2 , and c_3 follow from the boundary conditions and can be calculated as

$$c_1 = \mathcal{Y}''_C(0) + \hat{\alpha}^2 \mathcal{Y}_C(0) = -E_0,$$

$$c_2 = \mathcal{Y}'''_C(0) + \hat{\alpha}^2 \mathcal{Y}'_C(0) = 0,$$

$$c_3 = \frac{1}{2} [\mathcal{Y}''''_C(0) + \hat{\alpha}^2 \mathcal{Y}''_C(0)] = \frac{1}{2} [\hat{\alpha}^2 E_0 + \hat{\alpha}^2 (-E_0)] = 0.$$

The values of $\mathcal{Y}'''_C(0)$ and $\mathcal{Y}''''_C(0)$ are found as follows. Equation (10) can be differentiated with respect to t_0 and yields

$$\dot{Y}'(t_0, t) + \alpha^2 Y'(t_0, t) - \alpha^2 \tilde{N}_i'(t_0, t) = 0, \quad (26)$$

$$-\mathcal{Y}''''(X) - \alpha^2 \mathcal{Y}''(X) - \alpha^2 \mathcal{N}(X) = 0. \quad (27)$$

Equation (26) can be differentiated a second time with respect to t_0 . In the stationary case this reads

$$\mathcal{Y}''''(X) + \alpha^2 \mathcal{Y}''(X) + \alpha^2 \mathcal{N}(X) = 0. \quad (28)$$

Using the above equations and the boundary conditions in the case of co-injection, the constants c_1 , c_2 , and c_3 are fixed. It remains to be solved

$$\mathcal{Y}''_C(X) + \hat{\alpha}^2 \mathcal{Y}_C = -E_0. \quad (29)$$

The equilibrium solution in the case of a small electric field at the cathode is given by

$$\mathcal{Y}_C(X) = -\frac{E_0}{\hat{\alpha}^2} [1 - \cos \hat{\alpha} X]. \quad (30)$$

From Eq. (21) the corresponding stationary deviation from the ion injection density in the case of co-injection is given by

$$\mathcal{N}_C(X) = \hat{\mu} \mathcal{Y}'_C(X) = -\frac{\hat{\mu} E_0}{\hat{\alpha}} \sin \hat{\alpha} X. \quad (31)$$

This equilibrium solution differs from the result in [23] because a wrong implicit boundary condition for $\tilde{N}_i'(t_0, t_0)$ was used there.

In the case of counterstreaming electrons and ions, the constants c_1 , c_2 , and c_3 cannot be determined so easily, because two of the five boundary conditions are posed at the anode. Therefore the equilibrium solution is given by

$$\mathcal{Y}_A(X) = \frac{1}{\hat{\alpha}^2} (c_1 + c_2 X) + c_3 \left[\frac{X^2}{\hat{\alpha}^2} - \frac{2}{\hat{\alpha}^4} \right] + c_4 \cos \hat{\alpha} X + c_5 \sin \hat{\alpha} X, \quad (32)$$

which follows from an integration of (19). The boundary conditions have to be linearized up to $O(\epsilon)$ and $O(\hat{\mu}\epsilon)$ to keep the problem solvable. We assume that $\epsilon < \hat{\mu} \ll 1$ and quadratic and higher orders in ϵ and $\hat{\mu}$ are neglected. Strictly speaking, $Y_A(t_0, t)$ can be split into $Y_{A0}(t_0, t) + Y_{A1}(t_0, t)$ with $Y_{A0}(t_0, t)$ being of $O(\epsilon)$ and $Y_{A1}(t_0, t)$ of $O(\hat{\mu}\epsilon)$. From Eq. (21) it follows that $\tilde{N}_i'(t_0, t)$ is $O(\hat{\mu}\epsilon)$.

The boundary conditions (23) yield three linear equations for c_1, \dots, c_5 . Completing the system, the conditions (24) must be linearized. From the transit time condition it follows that for small electric fields $T = T_0 + \delta T$ [where $T_0 = 1$ and δT is of $O(\epsilon)$]. The contribution of the small deviation in the transit time leads, however, to corrections in quadratic order in ϵ and can therefore be neglected. Finally, we get

$$\begin{aligned} c_1 &= -E_0, \\ c_2 &= -\hat{\mu}\hat{\alpha}E_0\sin\hat{\alpha}, \end{aligned}$$

$$\begin{aligned} c_3 &= 0, \\ c_4 &= \frac{E_0}{\hat{\alpha}^2}, \\ c_5 &= \hat{\mu}\frac{E_0}{\hat{\alpha}^2}\sin\hat{\alpha}. \end{aligned}$$

We express the constants in this form containing $\hat{\mu}$ in $\hat{\alpha} = \alpha\sqrt{1 + \hat{\mu}}$, using (32) and linearizing the equilibrium solution for counterstreaming species afterwards. We find

$$\begin{aligned} \mathcal{Y}_A(X) &= -\frac{E_0}{\hat{\alpha}^2} \{1 - \cos\hat{\alpha}X + \hat{\mu}\sin(\hat{\alpha})[\hat{\alpha}X - \sin\hat{\alpha}X]\} + \dots \\ &= -\frac{E_0}{\alpha^2} (1 - \cos\alpha X) - \frac{E_0\hat{\mu}}{\alpha^2} \left\{ \frac{\alpha X}{2} \sin\alpha X + \sin(\alpha)[\alpha X - \sin\alpha X] - 1 + \cos\alpha X \right\} + O(\hat{\mu}^2\epsilon) + O(\hat{\mu}\epsilon^2). \end{aligned} \quad (33)$$

The additional terms in $O(\hat{\mu}\epsilon)$ in comparison to the result in the case of co-injection (30) are due to the different locations of the ion injection. The deviation in the ion fluid density from the injection density is given by

$$\begin{aligned} \mathcal{N}_A(X) &= \hat{\mu}[\mathcal{Y}'(X) - \mathcal{Y}'(1)] + \dots \\ &= -\frac{E_0\hat{\mu}}{\hat{\alpha}}(\sin\hat{\alpha}X - \sin\hat{\alpha}) + \dots \\ &= -\frac{E_0\hat{\mu}}{\alpha}(\sin\alpha X - \sin\alpha) + O(\hat{\mu}^2\epsilon). \end{aligned} \quad (34)$$

In our treatment both injection solutions differ only slightly because of the assumed smallness of $\hat{\mu}$. If $\hat{\mu} \ll 1$ is lifted, equilibrium solutions for co-injected ions can be found [26] for arbitrary kinetic energy ratios and are described by (30) and (31). Our results for counterinjected ions indicate differences to this solution simply by extrapolating (33) and (34) to finite values of $\hat{\mu}$. In general, the equilibrium solutions have to fulfill further constraints. The allowed values of the electric field E_0 are restricted by two conditions. From the transit time condition (6) it follows for equilibria that

$$T + \mathcal{Y}(T) = 1 \quad (35)$$

and from the external circuit equation follows after an integration in the stationary case

$$-\frac{1}{2}[1 + \mathcal{Y}'(T)]^2 + \frac{1}{2} = \frac{E_0}{C}. \quad (36)$$

Note that from the external circuit elements only the capacity C influences the equilibrium solutions as already found by Lawson [13] and Kuhn and Hörhager [12]. $\mathcal{Y}'(X)$ is proportional to E_0 ; therefore $E_0 = 0$, $T = 1$ [which corresponds to the uniform equilibrium $\Phi(x) = 0$ in the diode] is always an equilibrium solution for all values of α . How the stability of this uniform solution is affected by counterstreaming ions is investigated in the next section.

IV. THE DISPERSION RELATION

The electric field at the cathode is assumed now to show a time dependence of the form $E_0(t) = \epsilon_0 \exp(\sigma t)$ which represents the perturbed electric field at the cathode. This dependency is transferred to $Y(t_0, t) = \exp(\sigma t)y(X)$ and $\tilde{N}_i(t_0, t) = \exp(\sigma t)\eta(X)$ with $X = t - t_0$. The derivatives of a function of the type $F(t_0, t) = \exp(\sigma t)f(X)$ are calculated as follows:

$$\begin{aligned} \dot{F}(t_0, t) &= \partial_t F(t_0, t) = \exp(\sigma t)(\sigma + \partial_X)f(X), \\ F'(t_0, t) &= \partial_{t_0} F(t_0, t) = \exp(\sigma t)(-\partial_X)f(X). \end{aligned}$$

Assuming that the ions are counterstreaming means that the value of \mathcal{A} is greater than 1. The limiting situation of initially resting ions, where \mathcal{A} becomes 1, is not included in this case because $\hat{\mu}$ would tend to infinity in this situation. Therefore the calculation is restricted to small values of α . The short circuit case with initially resting but mobile ions was treated in [16–21, 26]. External-circuit elements can easily be incorporated and the resulting extended dispersion relation numerically evaluated. The differential equation for $Y(t_0, t)$ transforms into

$$-\partial_X \hat{l} y(X) = 0 = -\hat{l} \partial_X y(X) \quad (37)$$

with

$$\hat{l} = [(\sigma + \partial_X)^2 + \alpha^2][\sigma + (1 - \mathcal{A})\partial_X]^2 + \alpha^2\mu(\sigma + \partial_X)^2,$$

which is a fourth order linear differential operator with constant coefficients. The corresponding equation for the ion density is

$$\hat{l} \eta(X) = 0. \quad (38)$$

As in the equilibrium case, the boundary conditions are used in a linearized form. The general solution of Eq. (38) can be found by the ansatz

$$\eta(X) = \sum_{i=1}^4 \eta_{0i} \exp(k_i X), \quad (39)$$

where k_i are the four nonzero roots of the indicial equations for (38). The exact roots can be found quickly with an algebraic mathematical computer language, but they are extremely lengthy. It would be too cumbersome to continue the calculations on this basis. Fortunately, a physical argument is helpful, namely, the small mass ratio. Thus we linearize the operator and the functions, a situation which is familiar from the corresponding situation in the case of co-injection.

$$\begin{aligned}\hat{l} &= \hat{l}_0 + \hat{l}_1, \\ y'(X) &= y'_0(X) + y'_1(X),\end{aligned}\quad (40)$$

with $\hat{l}_0 = (1 - \mathcal{A})^2 \hat{p}^2 \hat{q} \hat{q}^\diamond$ and $\hat{l}_1 = \alpha^2 \mu \hat{\delta}^2$, where we have defined

$$\begin{aligned}\hat{p}\bar{\sigma} + \partial_X &= \exp(-\bar{\sigma}X) \frac{d}{dX} \exp(\bar{\sigma}X), \\ \hat{q} &\equiv \sigma + i\alpha + \partial_X, \\ \hat{q}^\diamond &\equiv \sigma - i\alpha + \partial_X, \\ \hat{q}\hat{q}^\diamond &= \exp(-\sigma X) \left[\frac{d^2}{dX^2} + \alpha^2 \right] \exp(\sigma X), \\ \hat{\delta} &\equiv \sigma + \partial_X = \exp(-\sigma X) \frac{d}{dX} \exp(\sigma X),\end{aligned}\quad (41)$$

with $\bar{\sigma} = \sigma / (1 - \mathcal{A})$. Instead of (37) a corresponding equation which results from a division by $(1 - \mathcal{A})^2$ can be used. This elucidates that $\check{l}_0 \equiv (1 - \mathcal{A})^{-2} \hat{l}_0 = \hat{p}^2 \hat{q} \hat{q}^\diamond$ is of $O(1)$ and that $\check{l}_1 \equiv (1 - \mathcal{A})^{-2} \hat{l}_1 = \alpha^2 \hat{\mu} \hat{\delta}^2$ is of $O(\hat{\mu})$. As a consequence, in the lowest order we have to solve

$$\check{l}_0 y'_0(X) = 0. \quad (42)$$

The next order is

$$\check{l}_0 y'_1(X) + \check{l}_1 y'_0(X) = 0. \quad (43)$$

The ion density $\eta(X)$ is of $O(\hat{\mu}\epsilon)$; therefore in our linearization procedure it remains to solve

$$\check{l}_0 \eta(X) = 0. \quad (44)$$

The boundary conditions for $y_0(X)$ and $y_1(X)$ must be calculated separately.

From $Y(t_0, t_0) = 0$, $\dot{Y}(t_0, t_0) = 0$, $Y'(t_0, t_0) = -1$, and from $\dot{Y}(t_0, t_0) = -\epsilon_0 \exp(\sigma t_0)$ follows

$$y_0(0) = 0, \quad y_1(0) = 0, \quad (45)$$

$$y'_0(0) = 0, \quad y'_1(0) = 0, \quad (46)$$

$$y''_0(0) = -\epsilon_0, \quad y''_1(0) = 0. \quad (47)$$

In the case of counterstreaming electrons and ions, the variation in the ion injection velocity vanishes; this implies in the Lagrangian description $\tilde{N}_i(t - T, t) = 0$ and leads in connection with Eq. (26) and with the time dependent ansatz to (lowest and next order)

$$(\sigma^2 + \alpha^2) y'_0(1) + 2\sigma y''_0(1) + y'''_0(1) = 0, \quad \eta(1) = 0. \quad (48)$$

As seen in the foregoing equations, the contributions of the derivation in the transit time are of quadratic order in

ϵ and can therefore be neglected. The corresponding boundary conditions at the cathode [resulting from (26)] are

$$y'''_0(0) = 2\sigma\epsilon_0, \quad y'''_1(0) = -\alpha^2\eta(0). \quad (49)$$

From (18) it can be concluded that

$$\eta'(1) = \hat{\mu} [\sigma^2 y_0(1) + 2\sigma y'_0(1) + y''_0(1)]. \quad (50)$$

Therefore our equation system (42)–(44) is completed by the boundary conditions (45)–(50) and the connection between the two functions becomes

$$\begin{aligned}\eta(X) &= -\frac{1}{\alpha^2} [(\sigma + \partial_X)^2 + \alpha^2] y'(X), \\ (\bar{\sigma} + \partial_X)^2 \eta(X) &= \hat{\mu} (\sigma + \partial_X)^2 y'(X).\end{aligned}\quad (51)$$

The solution $y_0(X)$ can be found by integration. Finally, this leads to

$$y_0(X) = \frac{\epsilon_0}{\sigma^2 + \alpha^2} \left[\exp(-\sigma X) \left[\cos\alpha X + \frac{\sigma}{\alpha} \sin\alpha X \right] - 1 \right], \quad (52)$$

which describes electrostatic perturbations of the uniform equilibrium of the classical Pierce diode. In the case of co-injection an analogous result was found in the lowest order. This is due to \check{l}_0 , which contains no contributions of the ion dynamics. The next order cannot be solved by integration because of the special quality of the boundary conditions. In contrast to this analytical method of solving differential equations, use can be made of the fundamental system of the linear differential operator \check{l}_0 , which is given by

$$\begin{aligned}\Theta_{\check{l}_0} &= \{ \exp(-\bar{\sigma}X), X \exp(-\bar{\sigma}X), \exp(-\sigma X) \cos\alpha X, \\ &\quad \exp(-\sigma X) \sin\alpha X \}.\end{aligned}\quad (53)$$

Now the coupled system of (43) and (44) and the connection between both through

$$\eta(X) = -\frac{1}{\alpha^2} [(\sigma + \partial_X)^2 + \alpha^2] y'_1(X) \quad (54)$$

can only be solved in a closed manner because of the special quality of the boundary conditions. The already known result in the leading order of $y(X)$ can be used. It is to be noted that the contribution of $O(\epsilon)$ in the last equation vanishes with $y_0(X) = y_{0, \text{Pierce}}(X)$. Using this result and the alternative representations of the differential operators from Eq. (43) yields

$$\begin{aligned}\exp(-\bar{\sigma}X) \frac{d^2}{dX^2} \exp[(\bar{\sigma} - \sigma)X] \left[\frac{d^2}{dX^2} + \alpha^2 \right] \\ \times \exp(\sigma X) y'_1(X) = -\alpha^3 \hat{\mu} \epsilon_0 \exp(-\sigma X) \sin\alpha X.\end{aligned}\quad (55)$$

Here a successive integration can be performed, which finally leads to

$$y_1'(X) = a \cos(\alpha X) \exp(-\sigma X) + b \sin(\alpha X) \exp(-\sigma X) + \left[-\frac{A_1}{2\alpha} \right] X \cos(\alpha X) \exp(-\sigma X) \\ + \frac{A_2}{2\alpha} X \sin(\alpha X) \exp(-\sigma X) + \frac{C_2}{(\bar{\sigma} - \sigma)^2 + \alpha^2} X \exp(-\bar{\sigma} X) + \left[\frac{C_1}{(\bar{\sigma} - \sigma)^2 + \alpha^2} + \frac{2C_2(\bar{\sigma} - \sigma)}{[(\bar{\sigma} - \sigma)^2 + \alpha^2]^2} \right] \exp(-\bar{\sigma} X). \quad (56)$$

The constants A_1 and A_2 are abbreviations for

$$A_1 = \frac{\alpha^2 \hat{\mu} \epsilon_0}{[(\bar{\sigma} - \sigma)^2 + \alpha^2]^2} \alpha [-(\bar{\sigma} - \sigma)^2 + \alpha^2], \quad (57)$$

$$A_2 = \frac{\alpha^2 \hat{\mu} \epsilon_0}{[(\bar{\sigma} - \sigma)^2 + \alpha^2]^2} 2\alpha^2 (\bar{\sigma} - \sigma). \quad (58)$$

a and b are the constants belonging to the homogeneous solution of the intermediate stage

$$\left[\frac{d^2}{dX^2} + \alpha^2 \right] \exp(\sigma X) y_1'(X) = \dots,$$

and C_1 and C_2 are so far undetermined integration constants. Use of Eq. (54) leads to

$$\eta(X) = -\frac{1}{\alpha^2} [A_2 \cos(\alpha X) \exp(-\sigma X) \\ + A_1 \sin(\alpha X) \exp(-\sigma X) \\ + C_2 X \exp(-\bar{\sigma} X) + C_1 \exp(-\bar{\sigma} X)]. \quad (59)$$

In this context, it should be noted that $\eta(X)$ results in a linear combination of the functions of the fundamental system of \check{I}_0 , as expected from Eq. (44).

To determine the four constants a , b , C_1 , and C_2 the five boundary conditions in $O(\hat{\mu}\epsilon)$ (46)–(50) can be used. This is not a contradiction because Eq. (49) is redundant. The results are lengthy expressions which can be found in Appendix A. This and the following calculations were achieved with the help of MAPLE V [28]. One constant is still lacking; it is the integration constant C_0 and it is given by (45) (see Appendix A). So $y_1(X)$ can be calculated completely (see Appendix B). Finally, the dispersion relation can be determined. The two constraints, the transit time and external-circuit conditions must be fulfilled by the time dependent solution

$$x(t_0, t) = t - t_0 + Y(t_0, t) = X + \exp(\sigma t) y(X)$$

with $y(X) = [y_0(X) + y_1(X)]$. The external circuit condition reads with $E(t_0, t) = -\check{x}(t_0, t)$

$$\int_t^{t-(T_0+\delta T)} dt_0 (-\check{Y})(-1+Y') \\ = - \left[\bar{L} \frac{d^2}{dt^2} + R \frac{d}{dt} + \frac{1}{C} \right] E_0(t). \quad (60)$$

Neglecting terms of $O(\epsilon^2)$ and using the assumed time dependence of the electric field at the cathode, we obtain

$$\int_t^{t-T_0} dt_0 \check{Y}(t_0, t) = - \left[\bar{L} \sigma^2 + R \sigma + \frac{1}{C} \right] \epsilon_0 \exp(\sigma t). \quad (61)$$

Using $Y(t_0, t) = y(X) \exp(\sigma t)$ we obtain after an X integration

$$\sigma^2 \int_0^1 y(X) dX + 2\sigma y(1) + y'(1) = \left[\bar{L} \sigma^2 + R \sigma + \frac{1}{C} \right] \epsilon_0. \quad (62)$$

This leads to the final dispersion relation

$$-\frac{\alpha^2 \epsilon_0}{(\alpha^2 + \sigma^2)^2} D_{0, \text{Pierce}} + \sigma^2 \int_0^1 y_1(X) dX \\ + 2\sigma y_1(1) + y_1'(1) = \left[\bar{L} \sigma^2 + R \sigma + \frac{1}{C} \right] \epsilon_0. \quad (63)$$

$D_{0, \text{Pierce}}$ is familiar as the Pierce dispersion relation

$$D_{0, \text{Pierce}} = \sigma^2 \left[\frac{\sigma^2}{\alpha^2} + 1 \right] + 2\sigma \\ - \exp(-\sigma) \left[2\sigma \cos \alpha + \left[\frac{\sigma^2}{\alpha^2} - 1 \right] \alpha \sin \alpha \right]. \quad (64)$$

Note that Eq. (63) is valid for counterstreaming as well as for co-streaming species, only the corresponding $y_1(X)$ has to be used. The evaluation of the second part of the dispersion relation for counterstreaming species can be found in Appendix C.

V. NUMERICAL EVALUATION OF THE DISPERSION RELATION AND DISCUSSION

To learn about the ionic contributions to the diode dynamics for arbitrary velocities we need as a reference the familiar solutions [11,13,18–20] of the classical Pierce diode dispersion relation: Fig. 2. Figure 2(a) shows the real part of σ , the growth (respectively damping) rate, as a function of α , and Fig. 2(b) the corresponding imaginary part. Aperiodic solutions are represented by dashed lines, oscillatory ones by solid lines. The latter always appear as conjugate pairs. For $\alpha > \pi$ the diode exhibits instability except for small windows just below the odd values of α/π and for the isolated points $\alpha/\pi = 2, 4, \dots$. Points of $\sigma_R = 0$ indicate the transition from the stable uniform equilibrium to another stable solution. At $\alpha/\pi = 1, 3, 5, \dots$ we observe transcritical bifurcations from the uniform to a nonuniform equilibrium. The critical points $\alpha/\pi = 2, 4, \dots$, where a marginally stable equilibrium solution exists, mark the onset of an oscillatory instability. A subcritical Hopf bifurcation is found

at the lower border of the stable windows, e.g., at $\alpha/\pi \approx 2.90$ [11].

The case of initially resting ions $v_{i0} \equiv 0$ ($\mathcal{A} \equiv 1$) for a hydrogen plasma is depicted in Fig. 3. Again, Fig. 3(a) shows the real part and Fig. 3(b) the imaginary part of the complex growth rate as a function of α , whereas the different branches of the dispersion relation are plotted in Fig. 3(c), representing the complex σ plane. One recognizes four unstable oscillatory modes (dashed-dotted lines), the Pierce-Buneman modes. They lead to a complete destabilization of the uniform equilibrium in the diode for all values of α since σ_R is positive everywhere.

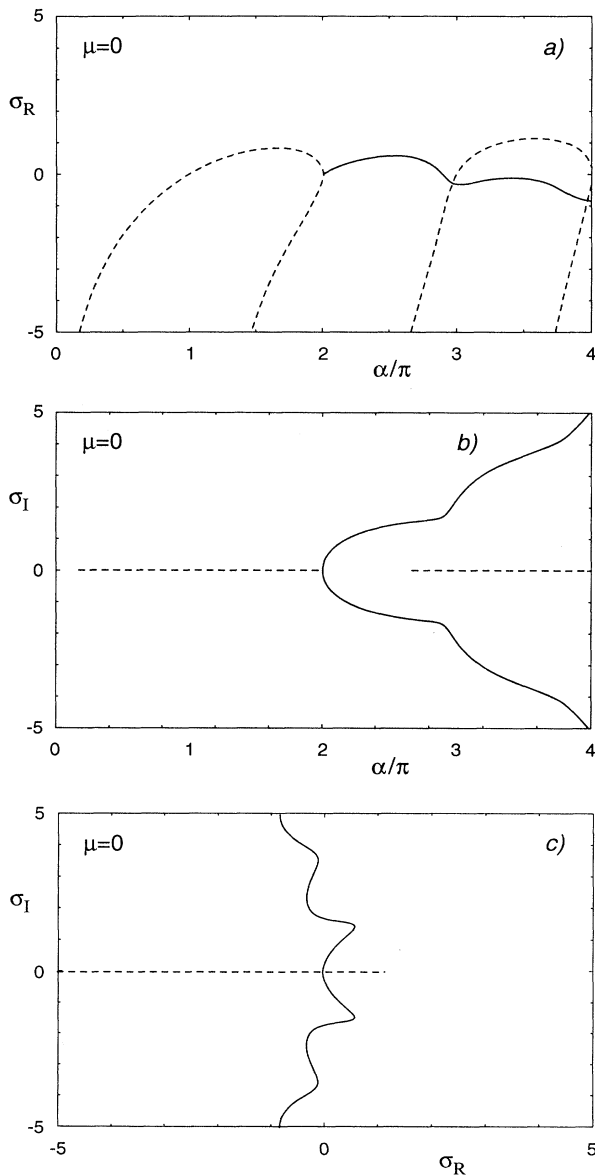


FIG. 2. Pierce case (immobile ion background, $\hat{\mu}=0$): growth rate σ_R (a) and frequency σ_I (b) of the solutions of the Pierce dispersion relation in the range $\sigma_R \in [-5, 5]$ and $\sigma_I \in [-5, 5]$. Dashed lines denote aperiodic, solid lines oscillatory solutions. (c) shows σ in the complex plane.

These oscillatory conjugate pairs show for higher α 's a bifurcation into two aperiodic growing modes, the first appearing for α slightly larger than π in the case of a hydrogen plasma [19,20]. The Pierce-Buneman modes form a butterfly wing pattern in the complex plane, Fig. 3(c).

The case of counterstreaming ions, $v_{i0} \leq 0$ ($\mathcal{A} \geq 1$) is shown for a hydrogen plasma in Fig. 4, where the growth rate σ_R is plotted as a function of the Pierce parameter for different values of $\mathcal{A} = 1 - v_{i0}/v_{e0} \geq 1$. Dashed-dotted lines represent oscillatory modes, solid lines aperiodic ones. Only the most unstable branches are depicted. For

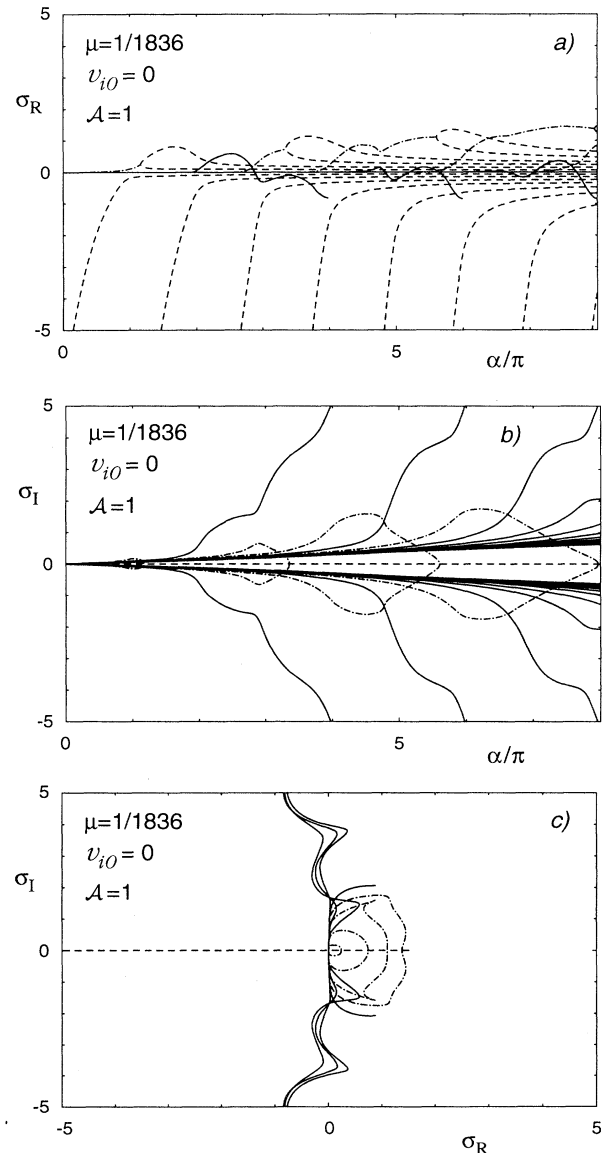


FIG. 3. Initially resting ions ($v_{i0}=0$, $\mathcal{A}=1$, hydrogen plasma): growth rate σ_R (a) and frequency σ_I (b) of the solutions of the dispersion relation in the range $\sigma_R \in [-5, 5]$ and $\sigma_I \in [-5, 5]$. (c) shows σ in the complex plane. The oscillatory modes (dashed-dotted lines) represent the Pierce-Buneman modes. In this case the diode becomes unstable for all values of α .

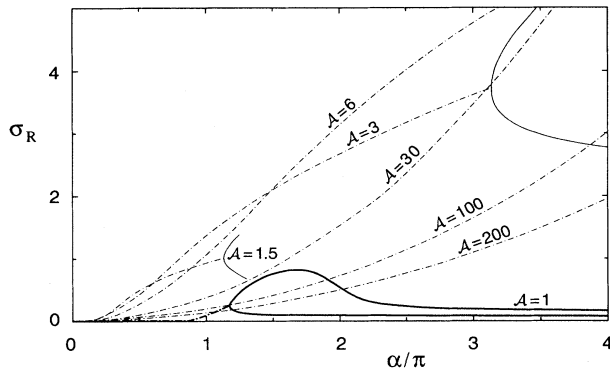


FIG. 4. The typical behavior of the new growing oscillatory branches (dashed-dotted lines) is displayed in the range of $0 < \alpha \leq 4\pi$ for distinct values of \mathcal{A} ($\mathcal{A} = 1 - v_{i0}/v_{e0}$) for a hydrogen plasma. For comparison, the case of initially resting ions, $\mathcal{A} = 1$, is depicted, too (bold line). These Pierce-Buneman modes for counterstreaming species exhibit an enhanced growth.

$\mathcal{A} = 1.5$ the two aperiodic branches have been cut for the sake of clarity. In each case the growth rate is monotonically increasing with α up to a bifurcation point, where two aperiodic branches appear. Generally this bifurcation point is shifted to larger values of α when \mathcal{A} is increased. In accordance with Fig. 3 we denote this oscillatory branch again the Pierce-Buneman branch. For $1.5 \lesssim \mathcal{A} \lesssim 20$ the growth rate of the Pierce-Buneman branch is an order of magnitude larger than in the case of initially resting ions ($\mathcal{A} = 1$; $v_{i0} = 0$). This dominance also holds in comparison with the other modes which we neglected in Fig. 4. This is seen in Figs. 5(a), 5(b), and 5(c) which show a completed dispersion diagram for a hydrogen plasma and $\mathcal{A} = 3$ ($v_{i0} = -2v_{e0}$). As in the co-moving case [26] the incorporation of ion dynamics leads to new modes and to new interconnections and bifurcations especially for the Pierce modes.

For all cases of $\mathcal{A} \geq 1$ the diode appears to be unstable in the whole α range. Counterstreaming of electrons and ions generally leads to a stronger destabilization of the diode with respect to the case of initially resting ions [20].

The question can be posed as to which mechanism stands behind this enhanced growth rate. An answer may be given by a Fourier mode analysis and by the feedback and coupling of these modes due to the presence of the two boundaries. This is elucidated by using an alternative derivation of the dispersion relation for normal modes as shown by Pierce [2] ($\mu = 0$) and by Kolyshkin, Kuznetsov, and Ender [20], ($\mu \neq 0$, $v_{i0} = 0$). A more general discussion can be found by Rognlén and Self [29].

This method makes use of a Fourier decomposition of the dependent Eulerian quantities and the linear dispersion relation of an unbounded plasma $D^\infty(\omega, k, \alpha) = 0$. The latter is resolved by $k_s(\omega, \alpha)$ where the index s' represents different branches. A superposition of these waves with complex coefficients allows one to satisfy the boundary conditions giving rise to the bounded plasma dispersion relation $D(\omega, \alpha) = 0$ which has solutions $\omega_s(\alpha)$, s again denoting different branches. Substituting

$\omega_s(\alpha)$ into $k_s(\omega(\alpha), \alpha)$ we obtain the associated wave numbers for forward and backward traveling waves.

The boundary conditions enforce a coupling between the linear modes with complex reflection coefficients which generally implies a change in amplitude and phase between the incident and the reflected waves at the boundaries. Following Kolyshkin, Kuznetsov, and Ender [20], this procedure is demonstrated more explicitly for

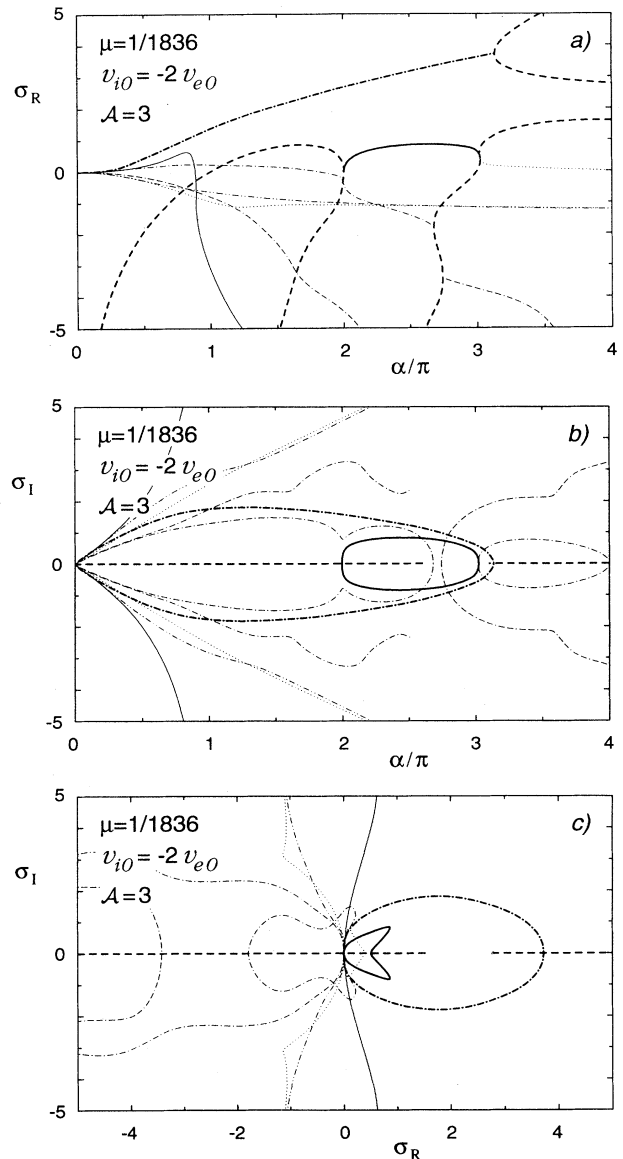


FIG. 5. Hydrogen plasma, $v_{i0} = -2v_{e0}$, $\mathcal{A} = 3$: growth rate σ_R (a) and frequency σ_I (b) of the solutions of the dispersion relation for counterstreaming species. (c) shows σ in the complex plane. Note the enhanced growth rate of the Pierce-Buneman branch (bold dashed-dotted line) compared with that of initially resting ions ($v_{i0} = 0$, Fig. 3). The bifurcation in two aperiodic growing modes takes place at $\alpha/\pi \approx 3.1$. The remaining bold lines denote the former Pierce branches (aperiodic, dashed lines, and oscillatory, solid lines). The thin lines are the new modes due to ion dynamics; dashed lines denote aperiodic branches.

initially resting ions ($v_{i0}=0$). We start with the dispersion relation for an unbounded plasma

$$1 - \frac{\omega_{pe}^2}{(\omega - kv_{e0})^2} - \frac{\omega_{pi}^2}{\omega^2} = 0, \quad (65)$$

where $\omega_{pi} = \mu^{1/2} \omega_{pe}$ is the ion plasma frequency. Normalizing frequency and wave number by v_{e0}/L and $1/L$, respectively, we get

$$D^\infty(\omega, k, \alpha) \equiv 1 - \frac{\alpha^2}{(\omega - k)^2} - \frac{\alpha^2 \mu}{\omega^2} = 0, \quad (66)$$

which is solved by

$$k_\pm = \omega \pm \beta(\omega; \alpha, \mu), \quad (67)$$

where

$$\beta(\omega, \alpha, \mu) = \frac{\alpha \omega}{\sqrt{\omega^2 - \alpha^2 \mu}}.$$

To meet the boundary conditions we have to superimpose these waves. The electric potential, for example, assumes the form

$$\begin{aligned} \phi(x, t) &= \exp(-i\omega t) [A_+ \exp(ik_+ x) + A_- \exp(ik_- x) + Bx] \\ &\equiv \exp(-i\omega t) \Phi(x), \end{aligned} \quad (68)$$

and similar expressions for the perturbed electron and ion density and velocity, respectively. Note that the third term reflects the boundedness of the plasma, being a special solution of the capacitor problem. The boundary conditions are that neither the total space charge nor the convection current are perturbed at the cathode. The former yields

$$k_+^2 A_+ + k_-^2 A_- = 0$$

and the latter

$$k_+ A_+ + k_- A_- = i \frac{(1 + \mu) \alpha^2}{\omega^2} B,$$

where B has been normalized by L^{-1} .

Both equations allow one to express A_+ and A_- linearly in terms of B so that $\Phi(x)$ can be written as $\Phi(x) = F(x, \omega; \alpha, \mu) B$ where the function F is given by Eq. (15) in [20]. The short circuit condition $\Phi(1) = 0$ finally yields

$$F(1, \omega; \alpha, \mu) \equiv D(\omega; \alpha, \mu) = 0, \quad (69)$$

the desired dispersion relation for initially resting ions. It coincides with that of [26] if ω is replaced by $i\sigma$. The normal modes are then given by the complex roots $\omega_s(\alpha, \mu)$ of (69). The "wave numbers" follow from (67) and become $k_\pm = \omega_s \pm \beta(\omega_s; \alpha, \mu)$. Generally k_+ and k_- turn out to be complex, being functions of α and μ , i.e., neither ω_s nor k_\pm are real quantities. Only in exceptional cases does the dimensional wave number \tilde{k}_\pm become real and can be identified with $\tilde{k}_\pm = \pm n\pi/L$ (e.g., for $\mu = 0$, $\alpha = n\pi$ we have $k_\pm = \pm n\pi$, $n = 1, 2, \dots$), as it is often used in attempts to interpret experimental results. The existence of two boundaries hence implies an intri-

cate coupling of the separate Fourier components of the unbounded theory, resulting in nonsymmetric, distorted spatial profiles of the eigenmodes (see also [1]). In contrast to periodic systems, no monochromatic real k value can be assigned and each bounded plasma system has to be followed individually [29].

Turning now to our problem of mobile ions with finite injection velocities, we first realize that v_{e0} and v_{i0} play an independent role through the loss of Galilean invariance. In an unbounded plasma instead only the relative velocity $v_{e0} - v_{i0}$ would enter.

The "unbounded" plasma dispersion relation therefore reads

$$1 - \frac{\omega_{pe}^2}{(\omega - kv_{e0})^2} - \frac{\omega_{pi}^2}{(\omega - kv_{i0})^2} = 0 \quad (70)$$

or in our normalization

$$D^\infty(\omega, k; \alpha, \mathcal{A}) = 1 - \frac{\alpha^2}{(\omega - k)^2} - \frac{\alpha^2 \mu}{(\omega - k \mathcal{A}^{-1})^2} = 0, \quad (71)$$

where $\mathcal{A} = 1 - A^{-1}$. This fourth order equation has now four roots k_s , $s' = 1, \dots, 4$, and accordingly the ansatz (68) has to be extended by two more complex coefficients. A unique solution is provided by two more boundary conditions, namely, no perturbed ion density and velocity at the ion injecting electrode. In principle, a replacement of the four coefficients A_1, \dots, A_4 in terms of B and of $k_1(\omega), \dots, k_4(\omega)$ could be imagined. However, already the roots $k_s(\omega)$ fill several pages, which renders the analysis impossible. The physical picture of forward and backward traveling waves with its intricate coupling drawn from the former example, however, can still be kept.

Our results then indicate that the counterstreaming of ions enhances this coupling providing a greater electrostatic feedback to the electron beam than do co-streaming ions. Intuitively counterstreaming ions are less able to neutralize electron density perturbations than co-moving ones. A detailed answer, of course, cannot be expected especially if one realizes that the normal mode frequencies (growth rates) are dependent in a complicated manner for a given Pierce parameter α on the mass ratio, the injection velocities, and the external-circuit conditions.

Our procedure based on the Lagrangian description of the electron fluid can equally well be interpreted in terms of superposed waves. Making the ansatz

$$x(t_0, t) = X + \exp(\sigma t) y(X), \quad (72)$$

where $X = t - t_0$, we arrive after a separation of the capacity mode at a fourth order differential equation for $y(X)$ (second order for initially resting ions [26] or for the Pierce case [26]). The four independent fundamental solutions correspond to the four Fourier modes, as also indicated by (39). The smallness of μ and the associated linearization keeps the problem solvable, as shown in the previous sections.

The main difficulty was that for ions injected from the

anode a mixed boundary value problem appeared [see (23) and (24) for the equilibrium case and (45)–(50) for the perturbation analysis] which could be solved up to $O(\mu^2)$.

In this paper an undriven diode was assumed and self-oscillations have been investigated. Growing solutions affect the whole diode region. This is reminiscent of an absolute instability [30–33]. On the other hand, elements of a convective instability are expected to occur for diodes which are driven periodically in time. This case as well as the nonlinear saturated state in case of instabilities are, however, beyond the intention of this paper.

Experimentally [4], in thermionic discharges at low pressures, the destabilization of the uniform potential region in the anode glow mode is found to coincide with a reversal of the ion velocities. In the light of the present results it is likely that this switch from co-moving to counterstreaming is responsible for the excitation of finite amplitude structures in the diode [34].

For real gas discharge systems, Kuhn [1] showed that the electrode sheath structure can under certain circumstances be incorporated as an external capacity in a Pierce model for a more realistic modeling of gas discharges. Now it is possible to incorporate ion dynamics with arbitrary ion velocities, too, in the search for a trigger mechanism for the destabilization of the uniform equilibrium in real gas discharge systems.

VI. SUMMARY AND CONCLUSIONS

The Lagrangian integral formulation presented in Sec. II gives a complete description of the stability of a Pierce-like diode with arbitrary velocities in as well as opposite to the direction of electron propagation. The similarities and differences of the two different cases of ion injection have been investigated with respect to equilibrium solutions and with respect to the stability behavior of the uniform equilibrium.

Equilibria for counterstreaming ions could be presented for small $\hat{\mu} = m_e v_{e0}^2 / m_i v_{i0}^2$. Extrapolation of our results to finite $\hat{\mu}$ is expected to yield substantial differences in the equilibrium solutions for the two injection conditions.

The linear stability analysis shows that the uniform equilibrium is unstable in the complete α range, where α is the Pierce parameter, if the species are counterstreaming, in contrast to co-moving beams, where stability is found up to $\hat{\alpha} = \pi$, where $\hat{\alpha} = \alpha \sqrt{1 + \hat{\mu}}$. In the case of

counterstreaming electrons and ions the dominant mode is oscillatory for not too large values of α and for all values of $|v_{i0}|$. They reduce to Pierce-Buneman modes known from the situation of initially resting ions. The diode with counterstreaming ions is found to be more unstable than for co-moving ions, the growth rate being an order of magnitude larger for $1.5 \leq \mathcal{A} \lesssim 20$, where $\mathcal{A} = 1 - v_{i0}/v_{e0}$, compared to the case $v_{i0} = 0$ ($\mathcal{A} = 1$, initially resting ions), with a maximum growth for $v_{i0} \approx -2v_{e0}$ in the case of a hydrogen plasma.

The integral formulation is found to be superior with respect to a Fourier mode analysis which anyway has to be modified substantially to meet the physics in a double bounded plasma. Caution is necessary when infinite plasma results are transferred to bounded plasmas.

Since in all plasma experiments boundaries are present, our model accounting for arbitrary motions between electrons and ions represents a valuable extension of the former models which are restricted to immobile or initially resting ions.

As long as kinetic effects are negligible or play a minor role and as long as there is a drift between species in a bounded plasma, the above investigations illuminate ion dynamical effects on the stability behavior on the electronic time scale. Usually the complex area of diode dynamics is governed by the dynamics of both species, introducing an intermittent type of dynamics where alternatively the electronic and the ionic time scales prevail. As long as kinetic effects are negligible or play a minor role, the hydrodynamic model can be a useful approach, e.g., in the theoretical modeling of low pressure gas discharges. In addition, it seems to be useful to extend the generalized Pierce diode model by kinetic effects, nonlinearities in E_0 and in the ion motion, particle reflections, and the appearance of virtual electrodes. With regard to inertial confinement fusion schemes [35], plasmoids [36], and thermionic converters [37] it seems desirable, too, to incorporate non-neutrality and a relativistic description.

ACKNOWLEDGMENT

One of the authors (H.K.) acknowledges support from the Graduiertenkolleg "Nonlinear Spectroscopy and Dynamics."

APPENDIX A: CONSTANTS a , b , C_1 , C_2 , and C_0

The constants a , b , C_1 , C_2 , and C_0 are given by

$$a = -\frac{C_1}{(\bar{\sigma} - \sigma)^2 + \alpha^2} - \frac{2C_2(\bar{\sigma} - \sigma)}{[(\bar{\sigma} - \sigma)^2 + \alpha^2]^2},$$

$$b = \frac{A_1}{2\alpha^2} + \frac{C_2[(\bar{\sigma} - \sigma)^2 - \alpha^2]}{\alpha[(\bar{\sigma} - \sigma)^2 + \alpha^2]^2} + \frac{c_1(\bar{\sigma} - \sigma)}{\alpha[(\bar{\sigma} - \sigma)^2 + \alpha^2]},$$

$$C_1 = \alpha^2 \hat{\mu} \epsilon_0 \left[\frac{c_{11} \alpha}{(\sigma^2 + \alpha^2)[(\bar{\sigma} - \sigma)^2 + \alpha^2]^2} \sin(\alpha) \exp(\bar{\sigma} - \sigma) \right. \\ \left. + \frac{c_{12} \alpha^2}{(\sigma^2 + \alpha^2)[(\bar{\sigma} - \sigma)^2 + \alpha^2]^2} \cos(\alpha) \exp(\bar{\sigma} - \sigma) - \frac{\sigma^2}{\sigma^2 + \alpha^2} \exp(\bar{\sigma}) \right],$$

$$c_{11} = \alpha^4(\bar{\sigma} + 1) + \alpha^2(\sigma\bar{\sigma}^2 - 2\bar{\sigma}\sigma + \bar{\sigma}^2 - \bar{\sigma}^3) + \sigma^4 + \sigma^4\bar{\sigma} - 3\sigma^3\bar{\sigma}^2 - 2\bar{\sigma}\sigma^3 + \bar{\sigma}^2\sigma^2 + 3\sigma^2\bar{\sigma}^3 - \bar{\sigma}^4\sigma,$$

$$c_{12} = \alpha^2(2\bar{\sigma}\sigma + 2\sigma - 2\bar{\sigma} - \bar{\sigma}^2) + 2\bar{\sigma}\sigma^3 + 2\sigma^3 - 5\bar{\sigma}^2\sigma^2 - 2\sigma^2\bar{\sigma} + 4\bar{\sigma}^3\sigma - \bar{\sigma}^4,$$

$$C_2 = \alpha^2\hat{\mu}\epsilon_0 \left[\frac{\alpha\bar{\sigma}}{(\sigma^2 + \alpha^2)[(\bar{\sigma} - \sigma)^2 + \alpha^2]} (\alpha^2 - 1 + \sigma\bar{\sigma}) \sin(\alpha) \exp(\bar{\sigma} - \sigma) \right. \\ \left. + \frac{\alpha^2\bar{\sigma}}{(\sigma^2 + \alpha^2)[(\bar{\sigma} - \sigma)^2 + \alpha^2]} (-2\sigma + \bar{\sigma}) \cos(\alpha) \exp(\bar{\sigma} - \sigma) + \frac{\sigma^2}{\sigma^2 + \alpha^2} \exp(\bar{\sigma}) \right],$$

$$C_0 = \frac{A_1\alpha}{(\sigma^2 + \alpha^2)^2} + \frac{C_2}{\bar{\sigma}^2(\sigma^2 + \alpha^2)} + \frac{C_1}{\bar{\sigma}(\sigma^2 + \alpha^2)} + \frac{\sigma A_2}{(\sigma^2 + \alpha^2)^2}.$$

The values of A_1 and A_2 can be found in (57) and (58).

APPENDIX B: $y_1(X)$

The solution $y_1(X)$ results from the integration of (56)

$$y_1(X) = \left[-\frac{\sigma A_1}{(\alpha^2 + \sigma^2)^2} - \frac{\sigma b}{\alpha^2 + \sigma^2} - \frac{(\sigma^2 - \alpha^2)A_2}{2\alpha(\alpha^2 + \sigma^2)^2} + \frac{\alpha a}{\alpha^2 + \sigma^2} \right] \sin(\alpha X) \exp(-\sigma X) \\ + \left[-\frac{\sigma A_2}{(\alpha^2 + \sigma^2)^2} - \frac{\sigma a}{\alpha^2 + \sigma^2} + \frac{(\sigma^2 - \alpha^2)A_1}{2\alpha(\alpha^2 + \sigma^2)^2} - \frac{\alpha b}{\alpha^2 + \sigma^2} \right] \cos(\alpha X) \exp(-\sigma X) \\ + \left[-\frac{A_2}{2(\alpha^2 + \sigma^2)} + \frac{\sigma A_1}{2\alpha(\alpha^2 + \sigma^2)} \right] X \cos(\alpha X) \exp(-\sigma X) \\ + \left[-\frac{A_1}{2(\alpha^2 + \sigma^2)} - \frac{\sigma A_2}{2\alpha(\alpha^2 + \sigma^2)} \right] X \sin(\alpha X) \exp(-\sigma X) - \frac{C_2}{\bar{\sigma}[(\bar{\sigma} - \sigma)^2 + \alpha^2]} X \exp(-\bar{\sigma} X) \\ + \left[-\frac{2C_2}{[(\bar{\sigma} - \sigma)^2 + \alpha^2]^2} - \frac{C_2}{\bar{\sigma}^2[(\bar{\sigma} - \sigma)^2 + \alpha^2]} + \frac{2\sigma C_2}{\bar{\sigma}[(\bar{\sigma} - \sigma)^2 + \alpha^2]^2} - \frac{C_1}{\bar{\sigma}[(\bar{\sigma} - \sigma)^2 + \alpha^2]} \right] \exp(-\bar{\sigma} X) + C_0$$

with the constants given in (57) and (58) and in Appendix A.

APPENDIX C: COMPLETION OF THE DISPERSION RELATION

$$d_0\sigma^2 \left[\frac{\sigma^2}{\alpha^2} + 1 \right] + 2\sigma - \exp(-\sigma) \left[2\sigma \cos(\alpha) + \left[\frac{\sigma^2}{\alpha^2} - 1 \right] \alpha \sin(\alpha) \right] \\ + \hat{\mu} [g_{11}d_{11} \sin(\alpha) \exp(\bar{\sigma} - \sigma) + g_{12}d_{12} \cos(\alpha) \exp(\bar{\sigma} - \sigma) + g_2d_2 \exp(\bar{\sigma}) + g_3d_3 \\ + g_{41}d_{41} (\sin\alpha)^2 \exp(\bar{\sigma} - 2\sigma) + g_{42}d_{42} \sin(\alpha) \cos(\alpha) \exp(\bar{\sigma} - 2\sigma) \\ + g_{43}d_{43} (\cos\alpha)^2 \exp(\bar{\sigma} - 2\sigma) + g_{51}d_{51} \sin(\alpha) \exp(-\sigma) + g_{52}d_{52} \cos(\alpha) \exp(-\sigma)] + d_{\text{cir}} \left[\bar{L}\sigma^2 + R\sigma + \frac{1}{C} \right] = 0 \quad (\text{C1})$$

with the following constants:

$$d_0 = -\bar{\sigma}^3(\sigma^2 + \alpha^2)[(\bar{\sigma} - \sigma)^2 + \alpha^2]^3,$$

$$d_{11} = \alpha\sigma\bar{\sigma}[(\bar{\sigma} - \sigma)^2 + \alpha^2],$$

$$d_{12} = \alpha^2\sigma\bar{\sigma}[(\bar{\sigma} - \sigma)^2 + \alpha^2],$$

$$d_2 = \sigma^3[(\bar{\sigma} - \sigma)^2 + \alpha^2]^3,$$

$$d_3 = \sigma[(\bar{\sigma} - \sigma)^2 + \alpha^2],$$

$$d_{41} = \alpha^2\bar{\sigma}^3,$$

$$d_{42} = \alpha^3\bar{\sigma}^3,$$

$$d_{43} = \alpha^4\bar{\sigma}^3,$$

$$d_{51} = \frac{1}{2}\alpha\bar{\sigma},$$

$$d_{52} = \frac{1}{2}\alpha^2\bar{\sigma},$$

$$d_{\text{cir}} = -(1/\alpha^2)\bar{\sigma}^3(\sigma^2 + \alpha^2)^3[(\bar{\sigma} - \sigma)^2 + \alpha^2]^3; \quad (\text{C2})$$

$$g_{11} = b_{11a}\alpha^6 + b_{11b}\alpha^4 + b_{11c}\alpha^2 + b_{11d},$$

$$b_{11a} = (-\bar{\sigma}^2 + \bar{\sigma} - 1)\sigma - 2\bar{\sigma}^2,$$

$$\begin{aligned}
b_{11b} &= (-\bar{\sigma}^2 + \bar{\sigma} - 1)\sigma^3 + (\bar{\sigma}^2 - \bar{\sigma} + 4)\sigma^2\bar{\sigma} \\
&\quad + (-10 + 4\bar{\sigma} - \bar{\sigma}^2)\sigma\bar{\sigma}^2 + 2(-\bar{\sigma} + 2)\bar{\sigma}^3, \\
b_{11c} &= (\bar{\sigma}^2 - \bar{\sigma} + 1)\sigma^5 + 2(-\bar{\sigma} + 2)\sigma^4\bar{\sigma}^2 \\
&\quad + (2\bar{\sigma}^2 + 10 - 14\bar{\sigma})\sigma^3\bar{\sigma}^2 \\
&\quad + (-\bar{\sigma}^2 + 13\bar{\sigma} - 12)\sigma^2\bar{\sigma}^3 + 3(1 - \bar{\sigma})\sigma\bar{\sigma}^4, \\
b_{11d} &= (\bar{\sigma}^2 + \bar{\sigma} + 1)\sigma^7 + (-3\bar{\sigma}^2 + 3\bar{\sigma} - 4)\sigma^6\bar{\sigma} \\
&\quad + (4 + 3\bar{\sigma}^2 - 2\bar{\sigma})\sigma^5\bar{\sigma}^2 \\
&\quad + (-\bar{\sigma} - 1)\sigma^4\bar{\sigma}^4 + (-1 + \bar{\sigma})\sigma^3\bar{\sigma}^4; \quad (C3)
\end{aligned}$$

$$\begin{aligned}
g_{12} &= b_{12a}\alpha^4 + b_{12b}\alpha^2 + b_{12c}, \\
b_{12a} &= 2(\bar{\sigma}^2 - \bar{\sigma} + 1)\sigma^2 + (-\bar{\sigma} + 5)\sigma\bar{\sigma}^2 - 2(1 + \bar{\sigma})\bar{\sigma}^2, \\
b_{12b} &= 4(\bar{\sigma}^2 - \bar{\sigma} + 1)\sigma^4 + 2(-3\bar{\sigma}^2 + 5\bar{\sigma} - 4)\sigma^3\bar{\sigma} \\
&\quad + 2(-9\bar{\sigma} + 2\bar{\sigma}^2 + 9)\sigma^2\bar{\sigma}^2 \\
&\quad + (-\bar{\sigma}^2 + 11\bar{\sigma} - 12)\sigma\bar{\sigma}^3 + 2(1 - \bar{\sigma})\bar{\sigma}^4, \\
b_{12c} &= 2(\bar{\sigma}^2 - \bar{\sigma} + 1)\sigma^6 + (-5\bar{\sigma}^2 + 5\bar{\sigma} - 8)\sigma^5\bar{\sigma} \\
&\quad + 4(\bar{\sigma}^2 + 1)\sigma^4\bar{\sigma}^2 \\
&\quad + (-\bar{\sigma}^2 - 5\bar{\sigma} + 4)\sigma^3\bar{\sigma}^3 + 2(-1 + \bar{\sigma})\sigma^2\bar{\sigma}^4; \quad (C4)
\end{aligned}$$

$$\begin{aligned}
g_2 &= b_{2a}\alpha^2 + b_{2b}, \\
b_{2a} &= (-\bar{\sigma}^2 + 2\bar{\sigma} - 2)(1 - \bar{\sigma})\bar{\sigma}, \\
b_{2b} &= (-\bar{\sigma}^2 + 2\bar{\sigma} - 2)\sigma^3; \quad (C5) \\
g_3 &= b_{3a}\alpha^6 + b_{3b}\alpha^4 b_{3c}\alpha^2 + b_{3d}, \\
b_{3a} &= (\sigma + 2)\bar{\sigma}^3 - 2\sigma^2\bar{\sigma} + 2\sigma^3, \\
b_{3b} &= 6(\sigma - 2\bar{\sigma})\sigma^4 + 2(-\bar{\sigma} + 6\bar{\sigma})\sigma^3\bar{\sigma}^2 \\
&\quad + 2(2\bar{\sigma} - 9)\sigma^2\bar{\sigma}^3 + (12 - \bar{\sigma})\sigma\bar{\sigma}^4 - 2\bar{\sigma}^5, \\
b_{3c} &= (-\sigma + 2)\sigma^2\bar{\sigma}^5 + 2(2\sigma - 1)\sigma^3\bar{\sigma}^4 \\
&\quad + 3(-\sigma - 4)\sigma^4\bar{\sigma}^3 + 6(4\bar{\sigma}^2 - 3\sigma\bar{\sigma} + \sigma^2)\sigma^5, \\
b_{3d} &= 2\sigma^5(\bar{\sigma} - \sigma)^4; \quad (C6)
\end{aligned}$$

$$\begin{aligned}
g_{41} &= b_{41a}\alpha^6 + b_{41b}\alpha^4 + b_{41c}\alpha^2 + b_{41d}, \\
b_{41a} &= 3(1 + \bar{\sigma})\sigma - (\bar{\sigma} + 2)\bar{\sigma}, \\
b_{41b} &= (-\bar{\sigma} - 1)\sigma^3 + 2(-\bar{\sigma} + 7)\sigma^2\bar{\sigma} \\
&\quad + 4(-3 + \bar{\sigma})\sigma\bar{\sigma}^2 + (-\bar{\sigma} + 2)\bar{\sigma}^3, \\
b_{41c} &= -\sigma(\bar{\sigma} - \sigma)(\bar{\sigma}^4 - 6\bar{\sigma}^3\sigma - \bar{\sigma}^3 + 8\bar{\sigma}^2\sigma^2 + 7\sigma\bar{\sigma}^2 \\
&\quad - 3\sigma^3\bar{\sigma} - 5\sigma^2\bar{\sigma} - 3\sigma^3),
\end{aligned}$$

$$\begin{aligned}
b_{41d} &= \sigma^3(\bar{\sigma}^2 - \bar{\sigma} - \bar{\sigma}\sigma - \sigma)(\bar{\sigma} - \sigma)^3; \quad (C7) \\
g_{42} &= b_{42a}\alpha^6 + b_{42b}\alpha^4 + b_{42c}\alpha^2 + b_{42d}, \\
b_{42a} &= 1 + \bar{\sigma}, \\
b_{42b} &= 3(-3\bar{\sigma} - 3)\sigma^2 + 3(2\bar{\sigma} + 6)\sigma\bar{\sigma} - 6\bar{\sigma}^2, \\
b_{42c} &= -5(1 + \bar{\sigma})\sigma^4 + 20(-1 + \bar{\sigma})\sigma^3\bar{\sigma} \\
&\quad + 12(-2\bar{\sigma} + 3)\sigma^2\bar{\sigma}^2 + 2(5\bar{\sigma} - 7)\sigma\bar{\sigma}^3 + (1 - \bar{\sigma})\bar{\sigma}^4, \\
b_{42d} &= \sigma^2(3\bar{\sigma}^3 - 8\sigma\bar{\sigma}^2 - 3\bar{\sigma}^2 + 5\sigma^2\bar{\sigma} \\
&\quad + 4\sigma\sigma + 5\sigma^2)(\bar{\sigma} - \sigma)^2; \quad (C8)
\end{aligned}$$

$$\begin{aligned}
g_{43} &= b_{43a}\alpha^4 + b_{43b}\alpha^2 + b_{43c}, \\
b_{43a} &= (-2 - 2\bar{\sigma})\sigma + (\bar{\sigma} + 2)\bar{\sigma}, \\
b_{43b} &= 4(1 + \bar{\sigma})\sigma^3 - 2(\bar{\sigma} + 8)\sigma^2\bar{\sigma} \\
&\quad + 2(-\bar{\sigma} + 6)\sigma\bar{\sigma}^2 + (\bar{\sigma} - 2)\bar{\sigma}^3, \\
b_{43c} &= \sigma(\bar{\sigma} - \sigma)(2\bar{\sigma}^4 - 2\bar{\sigma}^3 - 9\bar{\sigma}^3\sigma + 8\sigma\bar{\sigma}^2 + 13\bar{\sigma}^2\sigma^2 \\
&\quad - 4\sigma^2\bar{\sigma} - 6\sigma^3\bar{\sigma} - 6\sigma^3); \quad (C9)
\end{aligned}$$

$$\begin{aligned}
g_{51} &= b_{51a}\alpha^8 + b_{51b}\alpha^6 + b_{51c}\alpha^4 + b_{51d}\alpha^2 + b_{51e}, \\
b_{51a} &= (2\bar{\sigma} - 1 - 4\sigma)\bar{\sigma}^2 + 2\sigma^2, \\
b_{51b} &= -4(\bar{\sigma} + 3)\sigma^3\bar{\sigma} + 6\bar{\sigma}^4 + 4\sigma^4 - 2(3\bar{\sigma} + 10)\sigma\bar{\sigma}^3 \\
&\quad + 2(3\bar{\sigma} + 8)\sigma^2\bar{\sigma}^2 + 2\bar{\sigma}^5, \\
b_{51c} &= (2\sigma - 1)\bar{\sigma}^6 + 4(3 - 2\sigma)\sigma\bar{\sigma}^5 \\
&\quad + 12(\sigma - 2)\sigma^2\bar{\sigma}^4 - 2(5\sigma + 6)\sigma^3\bar{\sigma}^3 \\
&\quad + 2(19 + 2\sigma)\sigma^4\bar{\sigma}^2 - 12\sigma^5\bar{\sigma}, \\
b_{51d} &= 2\sigma^2(3\bar{\sigma}^4 + \sigma\bar{\sigma}^4 - 8\bar{\sigma}^3\sigma - 3\sigma^2\bar{\sigma}^3 + 2\bar{\sigma}^2\sigma^2 \\
&\quad + 2\sigma^3\bar{\sigma}^2 + 2\sigma^3\bar{\sigma} - 2\sigma^4)(\bar{\sigma} - \sigma)^2, \\
b_{51e} &= -\sigma^4(\bar{\sigma}^2 - 4\bar{\sigma}\sigma + 2\sigma^2)(\bar{\sigma} - \sigma)^4; \quad (C10)
\end{aligned}$$

$$\begin{aligned}
g_{52} &= b_{52a}\alpha^8 + b_{52b}\alpha^6 + b_{52c}\alpha^4 + b_{52d}\alpha^2 + b_{52e}, \\
b_{52a} &= -\bar{\sigma}^2, \\
b_{52b} &= -4\sigma^3 + 4\bar{\sigma}^2\sigma^2 + 4(-\bar{\sigma}^3 + \bar{\sigma}^2)\sigma - 4\bar{\sigma}^3, \\
b_{52c} &= -20(1 + \bar{\sigma})\sigma^3\bar{\sigma}^2 + 2(5\bar{\sigma} + 12)\sigma^4\bar{\sigma} - 12\sigma^5 \\
&\quad + 2(9\bar{\sigma} + 16)\sigma^2\bar{\sigma}^3 + 4\bar{\sigma}^5 - 8(\bar{\sigma} + 3)\sigma\bar{\sigma}^4 + \bar{\sigma}^6, \\
b_{52d} &= 4\sigma(\bar{\sigma} - \sigma)(\bar{\sigma}^5 - 4\sigma\bar{\sigma}^4 - \sigma^2\bar{\sigma}^4 + 2\sigma^3\bar{\sigma}^3 - \sigma^2\bar{\sigma}^3 \\
&\quad - \sigma^4\bar{\sigma}^2 + 12\sigma^3\bar{\sigma}^2 - 9\sigma^4\bar{\sigma} + 3\sigma^5), \\
b_{52e} &= -\sigma^3(\sigma\bar{\sigma}^2 + 4\bar{\sigma}^2 - 8\bar{\sigma}\sigma + 4\sigma^2)(\bar{\sigma} - \sigma)^4. \quad (C11)
\end{aligned}$$

- [1] S. Kuhn, *Phys. Fluids* **27**, 1821 (1984); **27**, 1834 (1984).
[2] J. R. Pierce, *J. Appl. Phys.* **15**, 721 (1944).
[3] F. Greiner, T. Klinger, and A. Piel, *Phys. Plasmas* **2**, 1810 (1995).
[4] T. Klinger, F. Greiner, A. Rohde, and A. Piel, *Phys. Plas-*

- mas* **2**, 1822 (1995).
[5] J. W. Poukey, J. P. Quintenz, and C. L. Olson, *J. Appl. Phys.* **52**, 3016 (1981).
[6] J. W. Poukey, J. P. Quintenz, and C. L. Olson, *Appl. Phys. Lett.* **38**, 20 (1981).

- [7] E. A. Coutsias and D. J. Sullivan, *Phys. Rev. A* **27**, 1535 (1983).
- [8] M. A. Raadu and M. B. Silevitch, *J. Appl. Phys.* **54**, 7192 (1983).
- [9] V. I. Kuznetsov and A. Ya. Ender, *Zh. Tekh. Fiz.* **47**, 2237 (1977) [*Sov. Phys. Tech. Phys.* **22**, 1295 (1977)]; **49**, 2176 (1979) [**24**, 1199 (1979)]; **51**, 2250 (1981) [**26**, 1326 (1981)]; **53**, 2329 (1983) [**28**, 1431 (1983)]; A. Ya. Ender, S. Kuhn, and V. I. Kuznetsov, in *Proceedings of the Fourth Symposium on Double Layers and Other Nonlinear Potential Structures in Plasmas, Innsbruck, Austria, 1992* (Institut für Theoretische Physica, Innsbruck, 1993), pp. 346–351.
- [10] M. A. Lampert and P. Mark, *Current Injection in Solids* (Academic, New York, 1970); E. Schöll, *Nonequilibrium Phase Transitions in Semiconductors* (Springer, Berlin, 1987).
- [11] B. B. Godfrey, *Phys. Fluids* **30**, 1553 (1987).
- [12] M. Hörhager and S. Kuhn, *Phys. Fluids B* **2**, 2741 (1990); S. Kuhn and M. Hörhager, *J. Appl. Phys.* **60**, 1952 (1986).
- [13] W. S. Lawson, *Phys. Fluids B* **1**, 1483 (1989); **1**, 1493 (1989).
- [14] T. L. Crystal and S. Kuhn, *Phys. Fluids* **28**, 2116 (1985).
- [15] J. Verboncœer, V. Vahedi, M. V. Alevs, and C. K. Birdsall, computer code PDP1, Plasma Device Planar 1-Dimensional Bounded Electrostatic Code (Plasma Physics and Simulation Group, University of California, Berkeley, 1990).
- [16] J. E. Faulkner and A. A. Ware, *J. Appl. Phys.* **40**, 366 (1969).
- [17] J. Frey and C. K. Birdsall, *J. Appl. Phys.* **36**, 2962 (1965).
- [18] K. Yuan, *J. Appl. Phys.* **48**, 133 (1977).
- [19] V. V. Vladimirov, A. N. Mosiyuk, and M. A. Mukhtarov, *Fiz. Plasmy* **9**, 992 (1983) [*Sov. J. Plasma Phys.* **9**, 578 (1983)].
- [20] I. N. Kolyshkin, V. I. Kuznetsov, and A. Ya. Énder, *Zh. Tekh. Fiz.* **54**, 1512 (1984) [*Sov. Phys. Tech. Phys.* **29**, 882 (1984)].
- [21] M. É. Gedalin, V. V. Krasnosel'skikh, and D. G. Lominadze, *Fiz. Plasmy* **11**, 870 (1985) [*Sov. J. Plasma Phys.* **11**, 508 (1985)].
- [22] S. Iizuka, K. Saeki, N. Sato, and Y. Hatta, *Phys. Rev. Lett.* **43**, 1404 (1979).
- [23] H. Schamel and V. Maslov, *Phys. Rev. Lett.* **70**, 1105 (1993).
- [24] H. Schamel and S. Bujarbarua, *Phys. Fluids B* **5**, 2278 (1993).
- [25] H. Kolinsky, MS thesis, University of Bayreuth, 1993.
- [26] H. Kolinsky and H. Schamel, *Phys. Plasmas* **1**, 2370 (1994).
- [27] S. Kuhn and M. Hörhager, *J. Appl. Phys.* **60**, 1952 (1986).
- [28] B. C. Char, K. O. Geddes, G. H. Gonnet, B. L. Leong, M. B. Monagan, and S. M. Watt, computer code MAPLE V, library reference manual, Waterloo Maple Software, 1991.
- [29] T. D. Rognlien and S. A. Self, *J. Plasma Phys.* **1**, 13 (1972).
- [30] R. Q. Twiss, *Proc. Phys. Soc. London Sect. B* **64**, 654 (1951); *Phys. Rev.* **84**, 448 (1951); **88**, 1392 (1952).
- [31] A. Bers and R. J. Briggs, *Bull. Am. Phys. Soc.* **9**, 304 (1964).
- [32] R. J. Briggs, Ph.D. thesis, MIT, Cambridge, MA, 1964.
- [33] A. Bers, in *Basic Plasma Physics I*, edited by A. A. Galeev and R.N. Sudan, *Handbook of Plasma Physics Vol. 1* (North-Holland, Amsterdam, 1983), Chap. 3.2, pp. 451–517.
- [34] F. Bauer and H. Schamel, *Physica D* **54**, 235 (1992).
- [35] D. S. Lemons and J. R. Cary, *J. Appl. Phys.* **53**, 4093 (1982).
- [36] G. F. Kiuttu and R. J. Adler, in *Microwave and Particle Beam Sources and Propagation*, SPIE Proc. Vol. 873 (SPIE, Bellingham, WA, 1988), pp. 256–263.
- [37] A. Ya. Ender (private communication).